1-19-2020

Analysis of surfactant-associated bacteria in the sea surface microlayer using deoxyribonucleic acid sequencing and synthetic aperture radar

Georgia Parks
Nova Southeastern University, georgiaparks3@gmail.com

Cayla W. Dean
Nova Southeastern University, cd821@nova.edu

John Alexander Kluge
Nova Southeastern University, jk1083@nova.edu

Alexander Soloviev
Nova Southeastern University, soloviev@nova.edu

Mahmood S. Shivji
Nova Southeastern University, mahmood@nova.edu

See next page for additional authors

NSUWorks Citation

Authors

Aurelien Tartar
Nova Southeastern University, aurelien@nova.edu

Kathryn L. Howe
Florida State University

Susanne Lehner
German Aerospace Center, susanne@dlr.de

Egbert Schwarz
German Aerospace Center

Hui Shen
Bedford Institute of Oceanography

William Perrie
Bedford Institute of Oceanography, William.Perrie@dfo-mpo.gc.ca

Paul Schuler
Oil Spill Response Limited, paulschuler@oilspillresponse.com
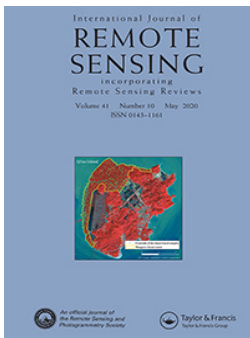
Analysis of surfactant-associated bacteria in the sea surface microlayer using deoxyribonucleic acid sequencing and synthetic aperture radar

Georgia Parks, Cayla W. Dean, John A. Kluge, Alexander V. Soloviev, Mahmood Shivji, Aurelien Tartar, Kathryn L. Howe, Susanne Lehner, Egbert Schwarz, Hui Shen, William Perrie & Paul Schuler

Taylor & Francis
Taylor & Francis Group

Analysis of surfactant-associated bacteria in the sea surface microlayer using deoxyribonucleic acid sequencing and synthetic aperture radar

Georgia Parks [a], Cayla W. Dean[a], John A. Kluge[a], Alexander V. Soloviev[a],
Mahmood Shivji[a], Aurelien Tartar[b], Kathryn L. Howe[c], Susanne Lehner[d], Egbert Schwarz[d],
Hui Shen[e], William Perrie[e] and Paul Schuler[f]

[a]Halmos College of Natural Sciences and Oceanography, Nova Southeastern University, Dania Beach, FL,
USA; [b]Department of Biological Sciences, Nova Southeastern University, Davie, FL, USA; [c]Department of
Earth, Ocean, and Atmospheric Science, Florida State University, Tallahassee, FL, USA; [d]Remote Sensing
Technology Institute, German Aerospace Center (DLR), Oberpfaffenhofen, Germany; [e]Ocean and Ecosystem
Sciences Division, Bedford Institute of Oceanography, Dartmouth, NS, Canada; [f]Oil Spill Response Limited,
Fort Lauderdale, FL, USA

ABSTRACT

The sea surface microlayer (SML) is the upper 1 mm of the ocean, where Earth's biogeochemical processes occur between the ocean and atmosphere. It is physicochemically distinct from the water below and highly variable in space and time due to changing physical conditions. Some microorganisms influence the composition of the SML by producing surfactants for biological functions that accumulate on the surface, decrease surface tension, and create slicks. Slicks can be visible to the eye and in synthetic aperture radar (SAR) satellite imagery. This study focuses on surfactant-associated bacteria in the near-surface layer and their role in slick formation where oil is present.

SML and subsurface water (SSW) samples were collected during the LAngrangian Submesoscale Experiment (LASER) experiment in February 2016 and the Submesoscale Processes and Lagrangian Analysis on the SHelf of Louisiana (SPLASH) experiment in April 2017 in the Gulf of Mexico, some near a known oil seep from a knocked down oil platform, during coordinated SAR overpasses. In most cases within slicks, results show a greater abundance of surfactant-associated bacteria in the SSW compared to the SML. This suggests that surfactants produced by these bacteria are transported to the sea surface via physical processes and accumulate in the SML. During the SPLASH project, surfactant-associated bacteria were also present in greater abundance in both the SML and SSW in oil slicks seen visually and from SAR than in areas where no oil was present. Bacteria capable of producing and degrading surfactants may influence oil degradation within these oil slicks. *In situ* observations can be used to verify and calibrate SAR satellite technology measurements, such as wind speed algorithms and slick identification. With global

coverage, SAR can be used to track organic material such as dissolved oil in the water column by the presence of surface slicks.

1. Introduction

The sea surface microlayer (SML) is an important boundary layer between the atmosphere and ocean. This interface is involved in global biogeochemistry processes such as air-water gas exchange, particle cycling, and microbial loops (Wurl et al. 2011). The SML is an extreme environment, exposed to turbulence, intense ultraviolet (UV) solar radiation, nutrient fluxes, and both temperature and salinity gradients. The composition of the SML was described by Hardy (1982) as a hydrophobic surfactant layer above 'wet' protein-polysaccharides, with a distinct layer of bacterioneuston below, which is defined as the community of bacteria within the SML. The revised, more accurate representation of the SML is a messier and more intimately arranged model consisting of a matrix of gelatinous particles and bacteria assemblages (Sieburth 1983; Cunliffe et al. 2013).

Franklin et al. (2005) proposed using membrane filters to collect samples from this layer for bacterial studies. Samples were collected from a small freshwater pond and sequenced using 16S (where S, Svedberg, is a unit of measurement) ribosomal ribonucleic acid (rRNA) gene clone libraries (Franklin et al. 2005). Kurata et al. (2016), Hamilton et al. (2015) and Howe et al. (2018) substantially advanced those techniques. The hydrophilic polycarbonate filter used in this study has a maximum sampling depth of 40μm, which falls within the boundaries defined by Soloviev and Lukas (2014), who describe the physical structure of the SML as a viscous sublayer (approximately 1500μm thick), thermal sublayer (approximately 500μm thick), and salinity diffusion sublayer (approximately 50μm thick). The structure of these layers is dependent on wind speed. When compared to work by Katsaros (1980) which states that the saline layer is approximately 200μm thick, Soloviev and Lukas (2014)'s estimates are only on the order of magnitude different and do not contradict. Under moderate wind speed conditions, these layers are controlled by gravity-capillary wave breaking and in turn impact gas exchange.

Biosurfactants are amphiphilic compounds (including peptides, fatty acids, phospholipids, glycolipids, antibiotics, and lipopeptides) produced by the bacterioneuston that can aid in the breakdown of oil (Karanth, Deo, and Veenanadig 1999). These natural surfactants are produced by the bacterioneuston for food capture, motility, protection, and aggregation (Cunliffe et al. 2013; Burch et al. 2010). These surfactants accumulate in the SML, forming slicks and modifying physical properties of the near-surface layer of the ocean by altering surface tension forces and damping short gravity-capillary waves, while also suppressing turbulence structures (Hühnerfuss and Garrett 1981; Soloviev et al. 2011). Sea slicks can affect gas exchange at the air–sea interface (Cunliffe, Upstill-Goddard, and Murrell 2011; Salter et al. 2011). Some common surfactant- and oil-associated bacteria genera are *Bacillus, Pseudomonas, Alcanivorax, Enterobacter, Halomonas, Rhodococcus, Marinobacter, Micrococcus*, and *Arthrobacter*.

Synthetic aperture radar (SAR) is an active remote sensing satellite that emits microwave signals that do not penetrate below the surface of the ocean but capture surface expression, enabling features such as internal waves, ship wakes, oil spills, ice, and convergence zones to be identified (Alpers and Hühnerfuss 1988; Gade et al. 2013). SAR is a sophisticated technology that has high ground resolution with pixel size on the metre

scale and the ability to penetrate cloud cover, and therefore works virtually in all weather conditions (including daytime and night-time) (Gade et al. 2013). The backscatter that SAR satellites measure is dependent on sea surface roughness, which has been related to wind speed (Lehner et al. 1998).

Additionally, surfactants have a damping effect on short gravity-capillary waves, or Bragg waves. As a result, slicks created by surfactants appear darker in relation to the surrounding rougher sea surface in SAR imagery (Alpers and Espedal 2004). Bright targets, or spots in the image, are commonly caused by man-made features such as oil rigs and ships. In this study, TerraSAR-X, RADARSAT-2, and Sentinel-1 satellites were used to visualize the presence of sea surface slicks, including those produced by oil spills. TerraSAR-X operates in X-band with dual polarization, RADARSAT-2 in C-band with quad polarization, and Sentinel-1in C-band with dual polarization.

In this work, we focus on the presence of surfactant-associated bacteria in slick areas. The purpose of this project is to further investigate the role of surfactant-associated bacteria in the SML, and the effect of wind speed and oil presence on the bacterioneuston. These observations will contribute to the current state of knowledge of the bacterioneuston, specifically those associated with surfactants and oil degradation. Because surfactants are essentially invisible to ocean colour satellite sensors, the use of SAR allows for the influence of surfactants to be observed by remote satellite sensors. The main motivation is to link SAR imaging with slicks associated with the presence of surfactant-associated bacteria (Soloviev and Lukas 2014; Hamilton et al. 2015; Kurata et al. 2016).

2. Materials and methods

2.1. Synthetic aperture radar data

For these studies, we utilized RADARSAT-2 satellite in Wide Scan mode, TerraSAR-X in Stripmap mode, and Sentinel-1in Interferometric Wide Swath mode (see Figures 1 and 4, and Tables 1 and 2). The reduced sea surface roughness due to slick presence results in reduced radar backscatter, which is interpreted as dark areas on the image. Slick presence is mainly dependent on wind speed and other parameters (surfactants, internal waves, fronts, oil spills, etc.). Vector wind field maps were calculated from SAR imagery (Figure 2(b), 3(c)).

2.2. In situ bacteria sampling

A total of 111 samples were collected in the Gulf of Mexico in February 2016 during the Gulf of Mexico Research Initiative-Consortium for Advanced Research on Transport of Hydrocarbon in the Environment (GoMRI-CARTHE) research cruise, LAngrangian Submesoscale Experiment (LASER) (Table 2). A total of 175 samples were collected in the Gulf of Mexico, some near a known oil seep from a damaged oil platform, in April 2017 during the GoMRI-CARTHE research cruise, Submesoscale Processes and Lagrangian Analysis on the SHelf of Louisiana (SPLASH) (Table 2). Figures 1 and 4 show sampling locations superimposed on the SAR imagery collected during these cruises. The measurement sites were selected based on the available ship time and the location inside of the pre-ordered SAR satellite image footprint. During LASER, sample collection occurred on a relatively large research vessel (R/V *F. G. Walton Smith*, with several groups competing for
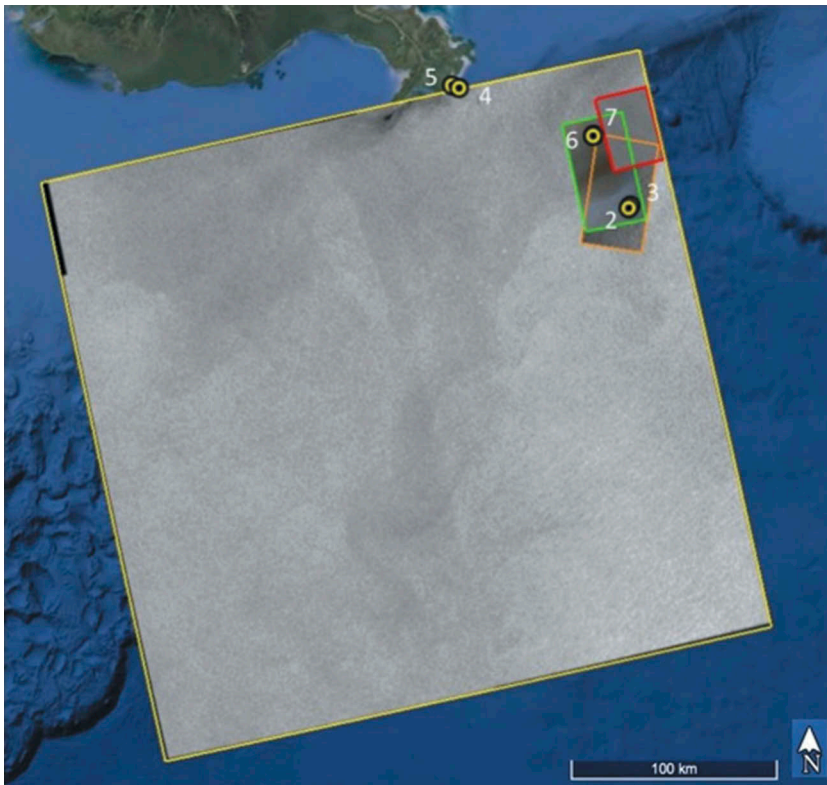
Figure 1. *In situ* sampling sites in the Gulf of Mexico during the 2016 LASER research cruise and SAR satellite images. The TerraSAR-X footprints are in orange (10 February) and green (11 February). The RADARSAT-2 footprints are in red (10 February) and yellow (13 February). The number of the sampling sites corresponding to Table 2 is also shown.

ship time. During SPLASH, a private small vessel (*Muy Loco*) was used and was devoted specifically to SML and subsurface water (SSW) sample collection, allowing for flexibility and increased number of samples collected during satellite overpass.

The sampling method was adapted from Franklin et al. (2005). Kurata et al. (2016) and Hamilton et al. (2015) implemented Franklin et al. (2005)'s method in the field and developed an approach that reduces contamination during sample collection. A 47-mm hydrophilic polycarbonate membrane filter that collects approximately 35 ± 5µm of the material was used to sample bacteria from the SML (Crow et al. 1975; Franklin et al. 2005). Compared to previous experiments by Kurata et al. (2016) and Hamilton et al. (2015), a greater number of samples were collected in this study, which increased the robustness of the statistical analysis. The filter sampling method also increases the efficiency of the collection in comparison to other SML sampling techniques.

Each SML filter was attached to a 10-foot fishing pole with a sterile hook and line and cast away from the boat and wake, reducing potential contamination. After resting on the water surface for a few seconds, the filter was lifted off and brought back to the boat and was placed directly into a sterile labelled MoBio bead tube (MoBio Laboratories, Inc., Carlsbad, CA), with sterile forceps and gloves. To collect SSW samples, a peristaltic pump

Table 1. SAR data collection information during the 2016 LASER and 2017 SPLASH research cruises. Local time of observations was Universal Time Coordinated (UTC)-5 hours. The polarization shown is for horizontal transmit and horizontal receive (HH), vertical transmit and vertical receive (VV), horizontal transmit and vertical receive (HV), and vertical transmit and horizontal receive (VH).

Cruise	Satellite	Date	Time (UTC)	Incidence angle (°)	Corner point coordinate	Dimension (km)	Polarization
LASER	TerraSAR-X	10 February 2016	12:00	24.810–27.990	28.73°N, 88.01°W 28.79°N, 88.33°W 28.23°N, 88.12°W 28.28°N, 88.44°W	32 × 57	VV
	RADARSAT-2	10 February 2016	23:44	18.380–20.380	28.95°N, 88.34°W 28.61°N, 88.26°W 28.66°N, 87.99°W 29.00°N, 88.07°W	300 × 300	VV
	TerraSAR-X	11 February 2016	23:49	29.540–32.480	28.33°N, 88.41°W 28.38°N, 88.10°W 28.84°N, 88.52°W 28.89°N, 88.20°W	30 × 50	VV
	RADARSAT-2	13 February 2016	23:57	19.300–39.530	28.62°N, 91.29°W 25.93°N, 90.64°W 26.50°N, 87.52°W 29.18°N, 88.10°W	25 × 25	VV
SPLASH	Sentinel-1	16 April 2017	1:30	30.669–46.127	27.95°N, 90.77°W 28.37°N, 88.19°W 29.46°N, 91.10°W 29.87°N, 88.49°W	250 × 170	VH/VV
	TerraSAR-X	19 April 2017	12:08	19.888–21.820	29.31°N, 89.74°W 29.28°N, 89.56°W 28.81°N, 89.85°W 28.78°N, 89.67°W	18 × 57	HH/VV
	TerraSAR-X	20 April 2017	23:57	42.649–43.844	29.17°N, 89.09°W 29.19°N, 88.93°W 28.66°N, 88.99°W 28.69°N, 88.83°W	16 × 56	HH/VV
	RADARSAT-2	20 April 2017	23:57	32.696–35.666	29.20°N, 89.32°W 29.20°N, 88.77°W 28.89°N, 89.32°W 28.89°N, 89.77°W	50 × 50	HH/VV HV/VH
	TerraSAR-X	25 April 2017	12:00	40.902–42.152	29.41°N, 90.06°W 29.41°N, 89.79°W 28.87°N, 90.06°W 28.87°N, 89.79°W	16 × 56	HH/VV

Table 2. In situ sample collection information during the 2016 LASER and 2017 SPLASH research cruises.

Cruise	Site	Date	Time (UTC)	Wind speed (m s⁻¹)	Number of SML samples	Number of SSW samples	Slick
LASER	2	6 February 2016	16:50	7–8	8	5	None
	3	6 February 2016	21:10	5–7	11	9	None
	4	10 February 2016	13:27	5–7	9	3	None
	5	10 February 2016	16:18	7–8	9	3	None
	6	12 February 2016	13:27	2–3	11	9	Intermittent
	7	12 February 2016	14:32	2–3	11	9	Yes
SPLASH	A	19 April 2017	11:22–12:45	4–5	13	9	None
	B	20 April 2017	14:11–15:31	6–8	10	10	None
	C	20 April 2017	15:54–16:50	6	12	9	Slick from oil
	D	21 April 2017	15:20–16:10	4	9	12	Slick from oil
	E	22 April 2017	12:09–13:10	2–3	18	10	Slick from oil
	F	22 April 2017	15:44–16:16	0–2	11	10	Intermittent, no visible oil
	G	25 April 2017	12:23–13:15	3–4	15	10	None
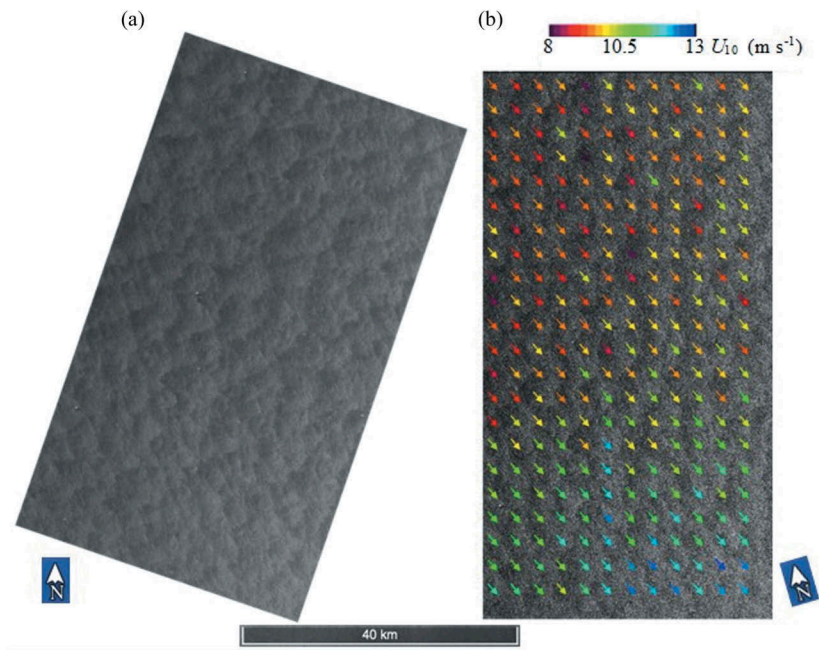
Figure 2. (a) The TerraSAR-X image acquired in VV on 10 February 2016 at 12:00 UTC, corresponding to the orange box in Figure 1. (b) The same TerraSAR-X image including spatial analysis of wind velocity. Wind speed is indicated by colour and vector direction.

was used from approximately 0.2-m depth into a sterile container on the boat. A filter was placed on the water surface in the container for a few seconds, then placed into a sterile labelled MoBio bead tube. Both SML and SSW filters were placed into MoBio deoxyribonucleic acid (DNA) tubes, which were used for DNA extraction, to reduce the loss of DNA material from the filter; only a small amount is collected during sampling with
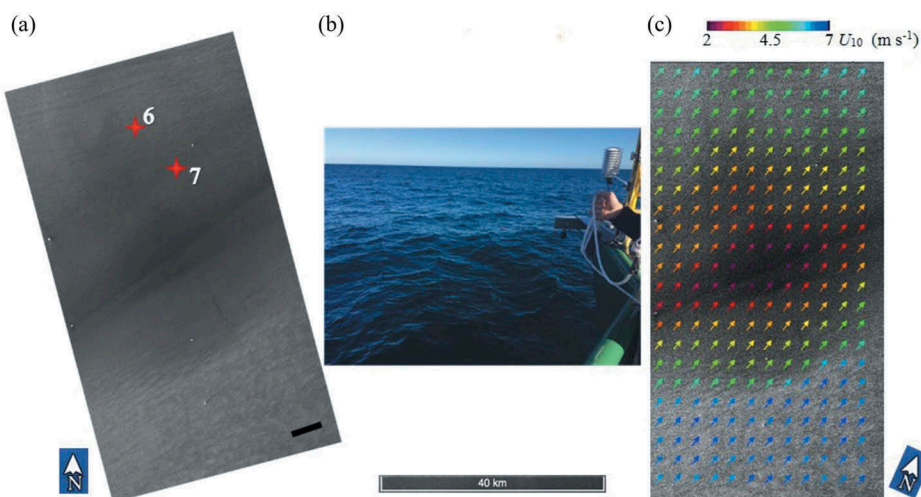
Figure 3. (a) The TerraSAR-X image acquired in VV on 11 February 2016 at 23:49:10 UTC with sampling Sites 6 and 7 the next morning, shown as red stars. Scale bar represents 5 km. (b) Photograph of the intermittent slick on 12 February 2016 during in situ microlayer sampling (Sites 6 and 7). (c) TerraSAR-X image including spatial analysis of wind velocity. Wind speed is indicated by colour and vector direction (Howe et al. 2018).
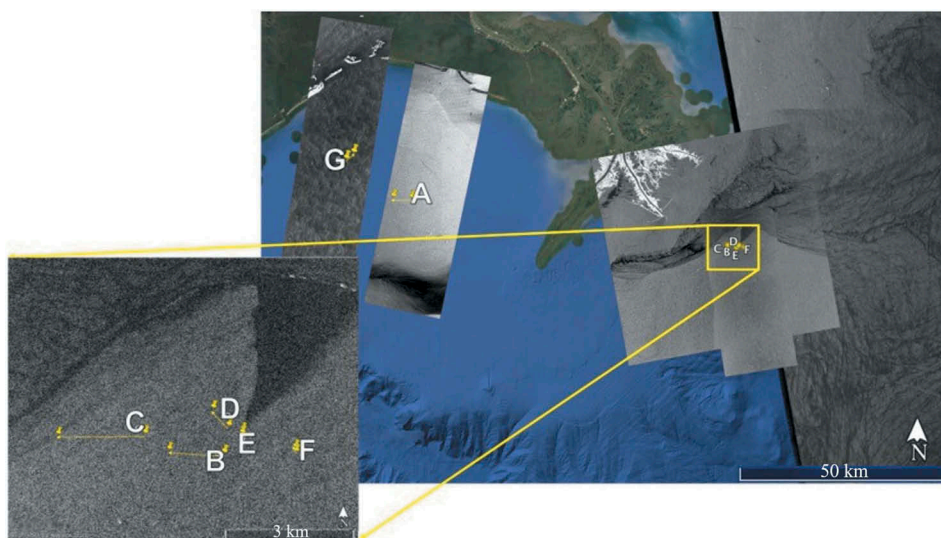
Figure 4. Sampling locations A-G from the SPLASH experiment in the Gulf of Mexico (Table 2). All SAR images taken over the course of the experiment are overlaid on the map. The small rectangular images are TerraSAR-X, the single square image is RADARSAT-2, and the largest image on the right side of the map is Sentinel-1.

polycarbonate membrane filters. All samples were immediately put on dry ice in the field, then transferred to a − 80°C freezer to store until DNA extraction.

To account for possible contamination by airborne bacteria during transportation from the sea surface to the MoBio bead tube, an air control (AC) sample was taken at each site.

For this purpose, a filter was exposed to the air for approximately 10 s with sterile forceps, then placed directly into the MoBio bead tube. Also, non-exposed (NE) control filters, which were only removed from their sterile containers during DNA extraction, served to estimate possible laboratory contamination. Sampling was recorded on a GoPro camera, which was later analysed to assess possible contamination. Wind speed measurements were recorded onboard at each sampling site.

2.3. Lab and bioinformatics

Subsequent DNA extraction was performed after sample collection in a sterile lab environment using the MoBio PowerWater DNA Isolation Kit and associated protocol. Twenty microlitres of extracted DNA of each sample were sent to Argonne National Laboratory (ANL) following standard protocol to be amplified and sequenced on the Illumina MiSeq™ platform on a 151–base pair (bp) × 12bp × 151bp MiSeq™ run, targeting the 16S rRNA gene using primers 515F and 806R (Caporaso et al. 2012). This followed the ANL amplification protocol of an initial denaturing step of 94°C for 3 min, 35 cycles of 94°C for 45 s, 50°C for 60s, and 72°C for 90s, and an extension at 72°C for 10 min. Using the bioinformatics pipeline, QIIME2™, the files output from sequencing were imported as EMP (Earth Microbiome Protocol) paired end sequences, demultiplexed and run through the Divisive Amplicon Denoising Algorithm 2 (DADA2) pipeline at a max error of 2.5, truncating at 150 reads and trimming at 12 reads, to denoise, dereplicate, and filter chimeras, creating amplicon sequence variants (ASVs) (Callahan et al. 2016). These ASVs are consistent labels with intrinsic biological meaning and are reusable across studies and reproducible in future datasets, defined as ≥97% 16S rRNA gene sequence similarity (Callahan, McMurdie, and Holmes 2017). Using Greengenes version 13.5, these ASVs were taxonomically classified (McDonald et al. 2012). Surfactant-associated genera were filtered and average abundance was calculated for each site. Averaging was done over consecutive samples on each of the sampling sites. The average for each genus of surfactant-associated bacteria was calculated by dividing the total number of ASV counts of each sample type at each site (i.e. SML at Site 1) by the number of samples collected at that type and site.

3. Results

3.1. Synthetic aperture radar and in situ measurements

The SAR images on 10 February 2016 (Figure 1) were collected during the LASER experiment under moderate wind speed conditions. During the experiment on 10 February 2016, no slicks were detected visually due to wind speeds above 5 m s^{-1} (Table 2). Neither TerraSAR-X nor RADARSAT-2 images showed slick presence on 10 February 2016 (Figure 1). The footprints of these images collected were not exactly over the sampling site on that day. Due to adverse weather conditions, the ship was sheltered behind a small island and was not able to get inside of the area of the satellite image.

The cellular structure seen in Figure 2(a) is most likely due to the strong atmospheric convection. Note that this was wintertime and the water was warmer than the air, while the cold, predominately northern wind came from the land (Figure 2(b)).

Slicks were observed visually on 12 February 2016 during *in situ* sampling (Figure 3(b)). The sampling conducted in low wind speed conditions of 2 m s^{-1} to 3 m s^{-1} on 12 February occurred 14 h after a TerraSAR-X satellite overpass on 11 February 2016 (Table 1). *In situ* sampling was not possible on 11 February 2016 in the area of the SAR overpass due to competition with other groups for use of the ship. Wind-wave conditions during the TerraSAR-X overpass shown in Figure 2 were similar to those on 12 February 2016, during *in situ* sampling. The TerraSAR-X Stripmap intensity image shows an area 30 km wide by 50 km long (Figure 3(a)). The slicks were seen in the SAR image and also seen visually from the R/V *F. G. Walton Smith*, which was in the footprint during the TerraSAR-X overpass on 11 February 2016.

There were well-defined convergence zones in the sampling area on 12 February 2016 (Figure 3(a)), supposedly related to a spiralling front (Wang and Özgökmen 2016). Convergence zones associated with downwelling are known for the accumulation of organic matter and microbial life (Espedal, Johannessen, and Knulst 1996). The dark elongated area and surrounding dark areas in the middle of the SAR image could indicate the presence of a slick in the frontal area. The lighter area at the bottom of the image is rougher water and indicates the presence of atmospheric convective cells due to warmer temperatures on the southern side of the front. Oil rigs appear in this image as bright spots. Wind speed (U_{10}) and direction have been calculated using sea surface roughness as determined from this SAR image (Figure 3(c)). Features seen during the LASER experiment were not associated with oil, whereas samples collected during the SPLASH project were located near a known oil seep, which is seen in Figure 4 in the SAR image.

The TerraSAR-X Stripmap image was taken while sampling was in progress at Site A on 19 April 2017 during the SPLASH experiment (Figure 4). There were no slicks visible by eye during sampling, which was confirmed by the lack of any clear dark slick-like feature in the image between the start and end coordinates. The TerraSAR-X Stripmap image taken on 20 April 2017 was taken approximately 8 h after sampling occurred at Site B and 14 h before sampling occurred at Sites C and D, shown as the inset SAR image (Figure 4). The distinct dark v-shaped feature indicates the surface expression of oil seeping from the damaged oil platform and a distinct front, confirmed by *in situ* observation. Samples were collected in a relatively small oil source area. At the same time, the SAR image showed a much wider slick. The discrepancy between the slick as seen visually and in SAR imagery was likely due to the presence of a very thin monomolecular layer suppressing short-gravity capillary waves. We did not collect samples outside the relatively narrow source area, as no oil was visually detected. The Sentinel-1 image to the right shows surface features associated with a frontal feature spreading throughout the Gulf of Mexico.

3.2. DNA analysis of bacteria

Repeated samples show comparable numbers of ASVs for each genus investigated within each site. To address any minor variability between repeated samples, data were normalized by averaging the total counts of ASVs for each genus of bacteria in the samples by the number of samples collected at each site. Discussion and conclusions were based on in-depth analysis with confidence intervals performed on each genus of surfactant-associated bacteria of interest to address this variation. Due to the natural variability of microbial communities and sea slicks in time and space, it is necessary to determine what is natural
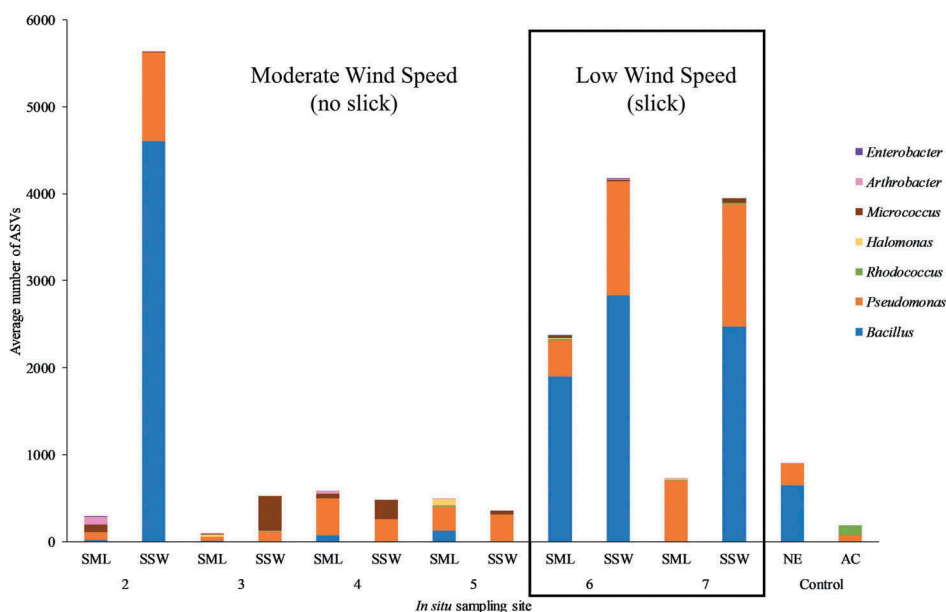
Figure 5. LASER results showing average ASVs per site for surfactant-associated bacterial genera.

variation and what is contamination. Because of this natural variability, only samples without substantial contamination or recorded interference during collection (*i.e.* touching an arm, folding, etc.) were included in analysis. Illumina MiSeq™ DNA sequencing provides the opportunity to analyse thousands of genera of bacteria and provide more robust results, as compared to the analysis of the same data with quantitative PCR analysis (Howe et al. 2018). Using QIIME2™, 1,103 bacteria genera were identified out of 12,720 ASVs from 9,376,004 sequences generated from the LASER data, and 1,054 bacteria genera were identified out of 11,693 ASVs from 8,079,507 sequences generated from the SPLASH data. In order to eliminate contamination, surfactant- and oil-associated bacteria genera that were not present or low in abundance on NE and non-template control filters were selected for downstream analysis, which include *Bacillus, Pseudomonas, Alcanivorax, Marinobacter, Rhodococcus, Halomonas, Micrococcus, Arthrobacter*, and *Enterobacter* (Figure 5). It should be noted that *Marinobacter, Rhodococcus, Halomonas, Arthrobacter*, and *Enterobacter* were substantially less abundant compared to *Bacillus* and *Pseudomonas* during LASER. *Pseudomonas* was found in high abundance on the NE control filters during the SPLASH project and was excluded from this analysis. *Alcanivorax*, an oil-degrading genus of bacteria, was only found in samples from the SPLASH project. Bacterial abundance from LASER and SPLASH by genera is shown in Figures 5 and 6. The number of counts for surfactant- and oil-associated bacteria are small in comparison to the overall counts of other genera that were either non-surfactant-associated or do not exist yet in the taxonomy database, so absolute counts are more reliable than relative abundance for this type of analysis. To compare the number of ASV counts found in each sample across all sites, the total number of ASVs was averaged over each site and type by sample number to normalize results.
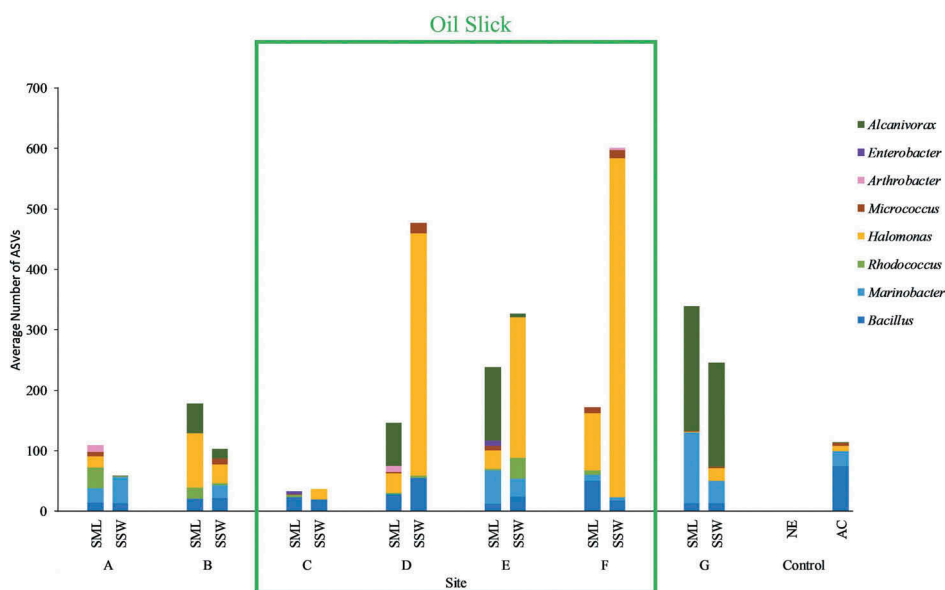
Figure 6. SPLASH results showing average ASVs per site for surfactant-associated bacterial genera. The data is separated by site on the x-axis, with type indicated within each site category. The green box outlines the four sites that were in an oil slick.

4. Discussion

In both SPLASH and LASER experiments, surfactant-associated bacteria were typically more abundant in the subsurface water (SSW) than in the sea surface microlayer (SML) within slicks and were more abundant in low wind speeds.

During the LASER experiment, on 6 February 2016 (Sites 2 and 3, see Figure 1) samples were collected under moderate wind speed conditions (Table 2). Both sites show a higher abundance of surfactant-associated bacteria in the SSW as compared to the SML (Figure 5). There was no SAR imagery taken on this date. On 10 February 2016 (Sites 4 and 5, see Figure 1), the samples were collected under moderate wind speed conditions (Table 2) near the Mississippi River Delta in brown water. No slicks were observed visually. There was no significant difference between SML and SSW in the samples collected on 10 February under moderate wind speed conditions. Notably, the abundance of surfactant-associated bacteria was relatively low in both the SML and SSW. A slick was observed during sampling on 12 February 2016 (Sites 6 and 7, Table 1, Figure 1). A slick was also seen in the TerraSAR-X imagery 12 h earlier (Figure 3). Site 6 samples were collected in an intermittent slick area. Site 7 samples were collected in a better-defined slick. In both cases, the SSW contained more surfactant-associated bacteria than the associated SML (Figure 5). Note that there was about 12 hours between the satellite overpass and the *in situ* sampling. The slick can change in time and space. At the time of the overpass, the slick was observed visually, but the ship was operating on a different project and *in situ* sampling was not possible until the morning of the next day.

During the SPLASH experiment, Sites A and G were located farthest away from the oil seep seen in the SAR image (Figure 4) and west of the Mississippi River outflow, and Sites B, C, D, E, and F were all located near the oil seep. Sampling at Site A occurred on 19 April

2017 and sampling at Site G occurred on 25 April 2017. No slicks were observed at either Sites A or G. Sampling at Sites B, C, D, E, and F all occurred from 20 to 22 April 2017 (Table 2, Figure 2). An oil sheen on the surface and the distinct smell of oil was observed *in situ* at Sites C, D, E, and F. Samples were collected from inside the relatively narrow oil source area, which was varying in location due to wind and currents, at each of these four sites (Figure 2). Surfactant- and oil-associated bacteria appear to be more abundant in the SSW than in the SML within the oil slicks (Figure 6).

It is noticeable that both *Marinobacter* and *Halomonas*, known surfactant-producing and oil-degrading genera of bacteria, were in significantly greater abundance in the SSW in samples from the oil slicks compared to areas outside of oil slicks in the SPLASH samples (Satpute et al. 2010) (Figure 6). *Alcanivorax*, another known surfactant-producing and oil-degrading genus of bacteria, was only found in the SPLASH samples associated with oil, and in significantly greater abundance in the SML in samples from the oil slicks (Satpute et al. 2010) (Figure 6). The lack of *Alcanivorax* in the LASER samples from the Gulf of Mexico, where oil was not detectable, suggests that the presence of these bacteria may be associated with oil. *Alcanivorax* was abundant in every sample collected at Site G from SPLASH, which is supposedly affected by the Mississippi River runoff. The water from the Mississippi River turns to the right by the Coriolis force and mostly enters the area west of the Mississippi Delta. We see the presence of *Alcanivorax* in all samples at Site G, which is west of the Mississippi Delta, and intermittently at Sites D and E, which are across the Mississippi Delta (Figures 4, 6). The LASER experiment was conducted east of the Mississippi Delta and did not reveal any *Alcanivorax* (Figures 1 and 5). In contrast, it is apparent that both surfactant-associated bacteria *Pseudomonas* and *Bacillus* (Satpute et al. 2010) were in greater abundance in the samples collected during LASER, where oil was not seen, than in the SPLASH samples (Figures 5, 6).

Wind speed was 6 m s^{-1} at Site C, between 2 and 4 m s^{-1} at Sites D, E, and G, and from 0 to 2 m s^{-1} at Site F (Table 2, Figure 4). This indicates that increasing wind speed has a negative effect on the abundance of oil-degrading bacteria within an oil slick, with lower wind speeds providing a more habitable environment for bacteria genera associated with oil and surfactants in both the microlayer and underlying water. At Site F during SPLASH, this relationship is the most distinct (Figure 4). The abundance of the bacteria is greatest in the SSW at Site F compared to any other site during SPLASH, which can be associated with the lowest wind speed. These findings support the idea that increased wind speed can prevent bacterioneuston from forming a stable community within the near surface layer (Rahlff et al. 2017).

The connection between sea surface roughness and wind speed in the presence of slick areas is not accounted for in the SAR wind speed algorithms. Though the SAR derived wind speed shows significant spatial variability over the dark slick area in Figure 3, the actual U_{10} may not change significantly over relatively small areas covered by surfactants. Note that on the SAR image collected at moderate wind speed and no slick conditions (Figure 2), the algorithm for wind speed calculation is expected to work well. However, in slick conditions, the algorithm shows a significant change in wind speed over a localized area, which may be an artefact due to the reduced sea surface roughness by the presence of surfactants. Wind speed was not derived from the images during SPLASH due to this condition, as the presence of oil inhibited an accurate calculation. A better understanding

of the connection between surfactant-associated bacteria and slicks may help in the development of better algorithms for wind measurements with radar scatterometers.

In this study, the number of successive SML samples was increased from a few in Kurata et al. (2016) and Hamilton et al. (2015) to as many as 10. A further increase of the number of successive samples above 10 is not feasible because the ship drifts and often leaves the slick area before completing the sampling set. In order to address seasonal and multi-year variability, long-term observations are needed, which is an opportunity for future research.

Although congregations of some bacteria (e.g. *Cyanobacteria*) can be seen from a satellite in colour imagery (Kahru 1997), congregations of surfactant-associated bacteria are not detectable in ocean colour satellite imagery. The use of SAR in this project instead enables the observation of slicks associated with these bacteria that can produce surfactants. SAR technology can help to visualize surfactant-derived slicks, which are formed due to bacteria processing organic material in the water column and production of surfactants. Further understanding of which microbial genera are capable of surfactant production is necessary to understand the processes associated with natural oil break down in the marine environment. SAR technology can thus be implemented to track organic material, such as dissolved oil and other biological materials in the water column, by the presence of surface slicks.

5. Conclusions

This manuscript is an advancement of the approach developed by Hamilton et al. (2015), Kurata et al. (2016), and Howe et al. (2018). Following the experience in LASER, where *in situ* measurements were conducted from a research vessel including several groups competing for the ship time, *in situ* measurements were done from a small boat in SPLASH, which provided more flexibility for coordination with satellite overpasses and significantly added to the SAR imaging statistics obtained during LASER. During SPLASH, microlayer samples were taken in the oil spill produced by the damaged and leaking Taylor Energy platform. We used next-generation sequencing Illumina MiSeq™, which broadened our analysis to over a thousand genera.

When combined, the seven surfactant-associated bacteria found in the LASER samples and the eight surfactant-associated bacteria found in the SPLASH samples were in greater abundance in the SSW than in the SML in natural and oil slicks in the Gulf of Mexico, which indicates that surfactants may be produced in SSW in the presence of organic materials or oil and transported to the SML via physical processes, accumulating on and enriching the SML. This occurs in slicks under low wind speed conditions but also in moderate wind speed conditions (see Figures 5 and 6 and Table 2). Samples collected outside of slicks (Sites 4 and 5 during LASER and Sites A, B, and G during SPLASH, see Figures 5 and 6) that were near or to the west of the Mississippi River Delta had a greater abundance of surfactant-associated bacteria in the SML than in the SSW. (Note that abundance of surfactant-associated bacteria was, in general, smaller under moderate wind speed conditions compared to low wind speed conditions). As the SML is a harsh environment impacted by wind, breaking waves, and UV rays, bacteria genera found in the SML samples are potentially more resistant and capable of surviving these factors. This work supports the importance of using SAR in coordination with *in situ* SML sample collection inside of slicks.

Bacteria capable of producing and degrading surfactants may have an important role in oil degradation within these oil slicks. The presence of oil-associated bacteria such as *Halomonas, Marinobacter*, and *Alcanivorax* in the slicks seen in SAR can distinguish between natural and oil-associated slicks. With global coverage, SAR can be used to track organic material such as dissolved oil in the water column by the presence of surface slicks.

Acknowledgements

Disclosure statement

No potential conflict of interest was reported by the authors.

Funding

ORCID

Georgia Parks (iD) http://orcid.org/0000-0003-3848-1690

References

Alpers, W., and H. A. Espedal. 2004. "Oils and Surfactants." *Synthetic Aperture Radar Marine User's Manual* 263–275. http://www.sarusersmanual.com/

Alpers, W., and H. Hühnerfuss. 1988. "Radar Signatures of Oil Films Floating on the Sea Surface and the Marangoni Effect." *Journal of Geophysical Research: Oceans* 93 (C4): 3642–3648. doi:10.1029/JC093iC04p03642.

Burch, A. Y., B. K. Shimada, P. J. Browne, and S. E. Lindow. 2010. "Novel High-throughput Detection Method to Assess Bacterial Surfactant Production." *Applied and Environmental Microbiology* 76 (16): 5363–5372. doi:10.1128/AEM.00592-10.

Callahan, B. J., P. J. McMurdie, and S. P. Holmes. 2017. "Exact Sequence Variants Should Replace Operational Taxonomic Units in Marker-gene Data Analysis." *The ISME Journal* 11 (12): 2639. doi:10.1038/ismej.2017.119.

Callahan, B. J., P. J. McMurdie, M. J. Rosen, A. W. Han, A. J. A. Johnson, and S. P. Holmes. 2016. "DADA2: High-resolution Sample Inference from Illumina Amplicon Data." *Nature Methods* 13 (7): 581. doi:10.1038/nmeth.3869.

Caporaso, J. G., C. L. Lauber, W. A. Walters, D. Berg-Lyons, J. Huntley, N. Fierer, S. M. Owens, J. Betley, L. Fraser, and M. Bauer. 2012. "Ultra-high-throughput Microbial Community Analysis on the Illumina HiSeq and MiSeq Platforms." *The ISME Journal* 6 (8): 1621. doi:10.1038/ismej.2012.8.

Caporaso, J. G., C. L. Lauber, W. A. Walters, D. Berg-Lyons, C. A. Lozupone, P. J. Turnbaugh, N. Fierer, and R. Knight. 2011. "Global Patterns of 16S rRNA Diversity at a Depth of Millions of Sequences per Sample." *Proceedings of the National Academy of Sciences* 108 (Supplement 1): 4516–4522. doi:10.1073/pnas.1000080107.

Crow, S. A., D. G. Ahearn, W. L. Cook, and A. W. Bourquin. 1975. "Densities of Bacteria and Fungi in Coastal Surface Films as Determined by a Membrane-adsorption Procedure 1, 2." *Limnology and Oceanography* 20 (4): 644–646. doi:10.4319/lo.1975.20.4.0644.

Cunliffe, M., R. C. Upstill-Goddard, and J. C. Murrell. 2011. "Microbiology of Aquatic Surface Microlayers." *FEMS Microbiol Reviews* 35 (2): 233–246. doi:10.1111/j.1574-6976.2010.00246.x.

Cunliffe, M., A. Engel, S. Frka, B. Gašparović, C. Guitart, J. Colin Murrell, M. Salter, C. Stolle, R. Upstill-Goddard, and O. Wurl. 2013. "Sea Surface Microlayers: A Unified Physicochemical and Biological Perspective of the Air–Ocean Interface." *Progress in Oceanography* 109: 104–116. doi:10.1016/j.pocean.2012.08.004.

Espedal, H. A., O. M. Johannessen, and J. Knulst. 1996. "Satellite Detection of Natural Films on the Ocean Surface." *Geophysical Research Letters* 23 (22): 3151–3154. doi:10.1029/96GL03009.

Franklin, M. P., I. R. McDonald, D. G. Bourne, N. J. P. Owens, R. C. Upstill-Goddard, and J. C. Murrell. 2005. "Bacterial Diversity in the Bacterioneuston (Sea Surface Microlayer): The Bacterioneuston through the Looking Glass." *Environmental Microbiology* 7 (5): 723–736. doi:10.1111/j.1462-2920.2004.00736.x.

Gade, M., V. Byfield, S. Ermakov, O. Lavrova, and L. Mitnik. 2013. "Slicks as Indicators for Marine Processes." *Oceanography* 26 (2): 138–149. doi:10.5670/oceanog.

Hamilton, B., C. Dean, N. Kurata, K. Vella, A. Soloviev, A. Tartar, M. Shivji, S. Matt, W. Perrie, and S. Lehner. 2015. "Surfactant-associated Bacteria in the Sea Surface Microlayer: Case Studies in the Straits of Florida and the Gulf of Mexico." *Canadian Journal of Remote Sensing* 41 (2): 135–143. doi:10.1080/07038992.2015.1048849.

Hardy, J. T. 1982. "The Sea Surface Microlayer: Biology, Chemistry and Anthropogenic Enrichment." *Progress in Oceanography* 11 (4): 307–328. doi:10.1016/0079-6611(82)90001-5.

Howe, K., C. W. Dean, J. A. Kluge, A. Soloviev, A. Tartar, M. S. Shivji, S. Lehner, and W. Perrie. 2018. "Relative Abundance of Bacillus Spp., Surfactant-associated Bacterium Present in a Natural Sea Slick Observed by Satellite SAR Imagery over the Gulf of Mexico." *Elementa: Science of the Anthropocene* 6: 1.

Hühnerfuss, H., and W. D. Garrett. 1981. "Experimental Sea Slicks: Their Practical Applications and Utilization for Basic Studies of Air-sea Interactions." *Journal of Geophysical Research: Oceans* 86 (C1): 439–447. doi:10.1029/JC086iC01p00439.

Kahru, M. 1997. "Using Satellites to Monitor Large-Scale Environmental Change: A Case Study of Cyanobacteria." *Monitoring Algal Blooms: New Techniques for Detecting Large-scale Environmental Change* 43: 45–47.

Karanth, N. G. K., P. G. Deo, and N. K. Veenanadig. 1999. "Microbial Production of Biosurfactants and Their Importance." *Current Science* 77: 116–126.

Katsaros, K. B. 1980. "The Aqueous Thermal Boundary Layer." *Boundary Layer Meteorology:* 18: 107–127. doi:10.1007/BF00117914.

Kurata, N., K. Vella, B. Hamilton, M. Shivji, A. Soloviev, S. Matt, A. Tartar, and W. Perrie. 2016. "Surfactant-associated Bacteria in the Near-surface Layer of the Ocean." *Scientific Reports* 6: 19123. doi:10.1038/srep19123.

Lehner, S., J. Horstmann, W. Koch, and W. Rosenthal. 1998. "Mesoscale Wind Measurements Using Recalibrated ERS SAR Images." *Journal of Geophysical Research: Oceans* 103 (C4): 7847–7856. doi:10.1029/97JC02726.

McDonald, D., M. N. Price, J. Goodrich, E. P. Nawrocki, T. Z. DeSantis, A. Probst, G. L. Andersen, et al. 2012. "An Improved Greengenes Taxonomy with Explicit Ranks for Ecological and Evolutionary Analyses of Bacteria and Archaea." *The ISME Journal* 6:610–618. doi:10.1038/ismej.2011.139.

Rahlff, J., C. Stolle, H.-A. Giebel, T. Brinkhoff, M. Ribas-Ribas, D. Hodapp, and O. Wurl. 2017. "High Wind Speeds Prevent Formation of a Distinct Bacterioneuston Community in the Sea-surface Microlayer." *FEMS Microbiology Ecology* 93 (5). doi:10.1093/femsec/fix041.

Salter, M. E., R. C. Upstill-Goddard, P. D. Nightingale, S. D. Archer, B. Blomquist, D. T. Ho, B. Huebert, P. Schlosser, and M. Yang. 2011. "Impact of an Artificial Surfactant Release on Air-sea Gas Fluxes during Deep Ocean Gas Exchange Experiment II." *Journal of Geophysical Research: Oceans* 116 (C11). doi:10.1029/2011jc007023.

Satpute, S. K., I. M. Banat, P. K. Dhakephalkar, A. G. Banpurkar, and B. A. Chopade. 2010. "Biosurfactants, Bioemulsifiers and Exopolysaccharides from Marine Microorganisms." *Biotechnology Advances* 28 (4): 436–450. doi:10.1016/j.biotechadv.2010.02.006.

Sieburth, J. M. 1983. "Microbiological and Organic-chemical Processes in the Surface and Mixed Layers." In *Air-sea Exchange of Gases and Particles*, 121–172. Dordrecht: Springer.

Soloviev, A., and R. Lukas. 2014. "Sea Surface Microlayer." In *The Near-Surface Layer of the Ocean*, 71–152. Dordrecht: Springer.

Soloviev, A., S. Matt, M. Gilman, H. Huhnerfuss, B. K. Haus, D. Jeong, I. Savelyev, and M. A. Donelan. 2011. "Modification of Turbulence at the Air-sea Interface Due to the Presence of Surfactants and Implications for Gas Exchange. Part I: Laboratory Experiment." In *Gas Transfer at Water Surfaces*, 245–258. Kyoto University Press.

Wang, P., and T. M. Özgökmen. 2016. "Spiral Inertial Waves Emitted from Geophysical Vortices." *Ocean Modelling* 99: 22–42. doi:10.1016/j.ocemod.2016.01.001.

Wurl, O., E. Wurl, L. Miller, K. Johnson, and S. Vagle. 2011. "Formation and Global Distribution of Sea-surface Microlayers." *Biogeosciences* 8 (1): 121–135. doi:10.5194/bg-8-121-2011.